

# Fully Automatic Segmentation of the Myocardium in Cardiac Perfusion MRI

Andreas Schöllhuber \*

VRVis Research Center  
Vienna, Austria

## Abstract

Reduced myocardial perfusion is an important indicator for coronary artery diseases. To perform early diagnosis the myocardial perfusion needs to be quantified. For this the myocardium has to be segmented in all time steps of the image sequence. Manually identification of myocardial boundaries is a very time consuming and tedious task. Existing automatic methods ignore motion artifacts, assumes that the heart is located at the center of the images, or requires user interactions to select a region of interest (ROI) covering the heart. Therefore, a fully automatic segmentation method is introduced in this work. This method uses spatial and temporal information and deals with motion artifacts. The ROI covering the heart is located by a hierarchical pattern matching algorithm. Motion artifacts are minimized by image registration using mutual information. Estimation of characteristic intensity-time curves followed by pixel-wise classification and boundary extraction deliver the final segmentation. The proposed method was successfully evaluated for 10 out of 11 data sets.

**Keywords:** Cardiac MRI, Perfusion, Segmentation, Registration, Mutual Information, Pattern Matching

## 1 Introduction

Cardiac perfusion MRI has been identified as a promising approach for preliminary detection of coronary artery diseases [2, 5, 18, 19]. Advantages of perfusion MRI compared to other perfusion imaging techniques such as SPECT or PET are: no radiation exposure, higher spatial resolution and higher availability. To visualize perfusion a contrast agent (CA) has to be administered intravenously. After some seconds (5-10sec) the CA appears in the right ventricle, followed by the left ventricle (after 10-15sec), and finally the myocardium (after 15-20sec)(figure 1). A myocardial ischemia is indicated by limited perfusion and therefore by a lower amount of contrast agent appearing in the myocardium. All these images are taken ECG gated i.e. all images are taken at the same stage of the cardiac cycle and on every heart beat. The whole acquisition time take about 40 seconds or more.

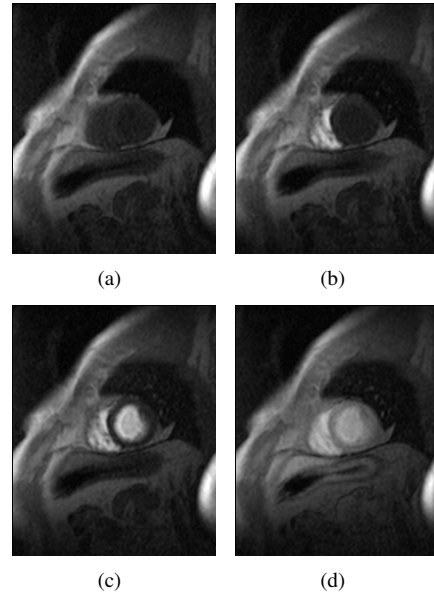


Figure 1: Perfusion Image Sequence. Before CA injection (a). After injection the CA first reaches the right ventricle (b), then the left ventricle (c) and finally the myocardium (d).

Currently the analysis of such perfusion images is done by manual inspection which is very time consuming. Therefore, a need for a robust and fully automatic analysis tool exists. Such a tool first has to segment the myocardium in all images and then calculate parameters to quantify the perfusion. This work focuses on automatic segmentation of the myocardium in perfusion MRI which is a very challenging task.

Automated segmentation of the myocardium in perfusion images is quite a difficult challenge. The complexity of this task is based on a wide range of image variabilities which are caused by patient movement, anatomy variations, pathologies, imaging noise and limited resolution as well as artifacts.

### Related Work

There exist only few methods for segmenting the myocardium in cardiac perfusion MRI. All of them hold some variabilities clearly out of mind or assume some human in-

\*schoell@vrvis.at

teractions.

Spreeuwets et al. [12, 13] have presented a method detecting myocardial boundaries based on image gray values. This method assumes that no motion artifacts are present or the images are already registered to each other. Pluempitiwiriyawej and Soththivirat [10] also ignore heart motions. Their method is based on active contours and extracts an initial contour which is passed to their so called stochastic active contour scheme (STACS) [9]. Adluru et al. [1] have shown another method based on level sets including an image registration step to reduce motion artifacts. This method however assumes that the heart is roughly located at the center of the images. Sun et. al [16] have presented a combination of contrast-invariant affine registration and segmentation. This method however requires human interaction to select a region of interest (ROI) at a reference image.

Different registration methods for perfusion images were presented. Stegmann et al. [14, 15] have shown a method for motion compensation by performing statistical analysis of annotated training data. Ólafsdóttir [7, 8] use an active appearance model (AAM) approach to minimize motion artifacts. Wong et al. [20] have shown a registration method based on normalized mutual information. Milles et al. [6] use a component analysis approach to extract image features for registration.

## Overview

This paper presents a fully automatic, three-step segmentation approach. First, the heart and a ROI covering it is detected automatically (section 2). Second, rigid registration is applied to minimize artifacts caused by patient motion (section 3). Third, the contours of the myocardium are extracted for every single time step (section 4).

## 2 Region of Interest

The first key task is to determine the region of interest (ROI). The ROI considered here is the image region covering the left ventricle and the myocardium.

As mentioned in the previous section ROI selection is often done manually. Typically the user has to define an area including the left ventricle by drawing a contour around it. The problem of automatic localization of the heart in non-perfusion MR images has been tackled by several authors by exploiting gray value variation over time [4, 11, 22]. We performed experiments using the above approach on perfusion data. For some datasets the method produced good results. However, it failed where larger motion artifacts appeared.

Therefore a new approach for detecting the heart in perfusion MRI is introduced. This novel method is based on a hierarchical approach of pattern matching of a very simple pattern of the left ventricle and the myocardium. The successive tasks (registration and segmentation) are then

exclusively performed on this ROI. This leads to better results and saves computation time.

In experiments we observed that motion artifacts and misaligned datasets are the major reasons disqualifying the mentioned variance based method for locating the heart in cardiac MRI perfusion data. Therefore we introduce an alternative method. This new method does not rely on gray value variations over time. Instead it tries to locate the heart in separate time steps. The new approach is based on pattern matching and pattern searching respectively in the whole dataset.

### Pattern Definition

The pattern that the algorithm is looking for represents the region of left ventricle and myocardium. The myocardium is seen as a circle with a range of possible diameters. It is assumed that the circle that has to be detected has a diameter between 40mm and 80mm. This approximately reflects the range of possible diameters for the left ventricle as observed in human anatomy [3]. The inner area of the circle represents the left ventricle.

Both areas - myocardium and left ventricle - are homogeneous regions and therefore we assume that the according gray value variances should be minimal. To ensure that these two homogeneous regions are different regions an additional constraint is added: the inner area has to be brighter than the circle itself. This leads to a detection of candidates where the contrast agent appears in the left ventricle and not yet in the myocardium.

The pattern we are basically looking for is a circle of homogeneous gray values surrounding a homogeneous region with different, brighter gray values. An exhaustive search of such a pattern would lead to unacceptable computation time.

### Pattern Matching (Multiple Candidates)

Therefore a hierarchical pattern matching algorithm is proposed to minimize computational costs. This hierarchical structure constricts the given pattern bit by bit and the amount of possible candidates decreases at every step.

We resume the individual constraints which are checked one after the other as the algorithm proceeds:

1. At the beginning every possible circle with a diameter between 40mm and 80mm is treated as a candidate. First the left point of a candidate is fixed (figure 2(a)).
2. The fixed point is compared to the right point (figure 2(b)). If the difference between these two pixels is lower or equal a given threshold (1% of gray value range) the candidate is kept otherwise it is discarded.
3. Now the upper and lower pixels of the candidates are considered. Since the left ventricle is not necessarily a perfect circle some variations of the upper and lower pixels are allowed. A  $3 \times 3$  neighborhood of

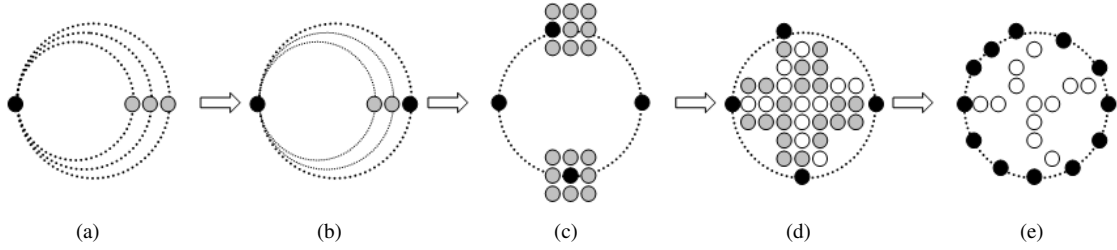


Figure 2: Pattern to match LV candidates

these pixels is taken into account and the pixel with the highest similarity to the left and right pixel is treated as upper and lower pixel respectively (figure 2(c)). The left and right pixels as well as the determined upper and lower pixels define the outer samples of the candidate. If the variance of these outer samples lies above a given threshold (0.1% of gray value range) the candidate is discarded.

4. After inspecting the contours of the candidates the inner areas are considered: samples in the neighborhood along the horizontal and the vertical axis are selected (figure 2(d)). These sample points (inner samples) must have a very high difference to the mean value of the outer samples to guarantee a good contrast.

To fulfill the constraint that the inner area (left ventricle) has to be brighter than the contour (myocardium) all candidates having a smaller mean value of the inner samples than the outer samples are discarded. To satisfy the other constraint - the inner area has to be homogeneous - all candidates with a high variance of the inner samples are discarded. This threshold is set to 0.5% of gray value range which is clearly higher than the variance threshold for the outer samples. This is due to the fact that the inner area of the matching model may include papillary muscles appearing darker than the contrast enhanced left ventricle. To further reduce the amount of candidates the difference between the mean values of the inner and outer samples has to be greater than a given threshold (30% of gray value range). Otherwise the candidate is discarded. This threshold seems to be very high but therefore only candidates having a very high contrast between outer (myocardium) and inner (left ventricle) samples will remain.

5. After identifying possible candidates more samples on the circle are taken (figure 2(e)) and the variance of the outer samples is recalculated to get a more robust measurement of the variance. This variance is used to indicate how well a candidate matches the pattern. A lower variance indicates a higher probability for being the correct candidate.

This hierarchical procedure filters out multiple candidates for each time step. Some of them do not represent

the left ventricle correctly due to misleading appearances of the pattern in the dataset. Therefore all candidates are sorted according to the variance of the outer samples and the ten candidates with lowest variance are kept. Typically some false positives remain.

### Pattern Matching (Best Candidate)

To finally identify the correct location of left ventricle and myocardium, a model matching approach is used introducing additional anatomical information. The model consists of two concentric circles and an attached circle segment (figure 3).

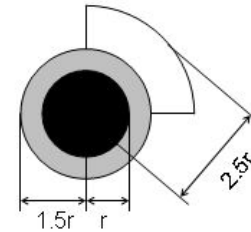


Figure 3: Model Left ventricle (black), myocardium (gray), lung (white)

The area inside the inner circle represents the left ventricle. The area between the two concentric circles represents the myocardium. The attached circle segment represents the lung and has an opening angle of  $90^\circ$ . These three regions are the most distinctive ones.

This model is placed on every candidate to identify the best one. It is placed in such a way that the centers of the candidate and the previously detected circle match. The radius of the model's left ventricle is set equal to the radius of the candidate. The thickness of the myocardium is chosen as half the radius of the candidate and the radius of the circle segment is set to 2.5 times the radius of the candidate.

To compare the candidates a difference measure has to be defined. We use the error rate according to the following classification. The assumption is made that the placed model correctly defines the three different regions (classes): LV, myocardium, and lung. The most likely assignment of gray values to classes is calculated. Afterward for every pixel under the model the expected class

based on the gray value is determined. For each pixel this gray value based classification is compared to the classification according to the region of the model that overlaps the pixel. All pixels for which the two classifications differ increase the difference measure between model and data. The error rate is defined as:

$$error\ rate = \frac{\#false\ classified\ samples}{\#samples} \quad (1)$$

The most likely assignment of a gray value  $g$  to a class  $c_i$  is defined as:

$$p(g|c_i) = \frac{H_{c_i}(g)}{\sum_{j=1}^N H_{c_i}(g_j)} \quad (2)$$

Whereas  $H_{c_i}(g)$  is the absolute frequency of the appearance of the gray value  $g$  in the class  $c_i$  and  $N$  indicates the number of available gray values. The expected class for a pixel with gray value  $g$  is determined by:

$$c = \arg\max_i p(g|c_i) \quad (3)$$

To deal with rotation the model is placed on the candidates and rotated in  $20^\circ$  steps. Finally the candidate with the lowest false classification ratio is identified as the best candidate (figure 7) and the bounding box covering the whole candidate is defined as the region of interest.

### 3 Registration

The relatively long data acquisition time of perfusion data - up to 40 seconds and more - leads to one major problem in the segmentation process: breathing artifacts. During the data acquisition process the patient is asked to hold the breath. However, not all patients are able to do so during the whole acquisition time. Breathing causes the lung to expand and contract. Due to the fact that the heart lies directly next to the lung it will change its position and shape. Since the segmentation relies on spatial and temporal information, it is essential to correct these motion artifacts as much as possible.

In order to eliminate motion artifacts the images of different time steps need to be registered. For this a similarity metric is required. Gray value difference, mean square error or cross correlation only lead to good results if all images exhibit similar gray values in corresponding regions. Perfusion images exhibit time-varying gray values due to enhancement caused by the contrast agent. For such images mutual information [17] is much better suited as difference measure. Mutual information of two discrete random variables  $X$  and  $Y$  is defined as:

$$I(X,Y) = \sum_{y \in Y} \sum_{x \in X} p(x,y) \cdot \log \frac{p(x,y)}{p(x) \cdot p(y)} \quad (4)$$

Here the two random variables  $X$  and  $Y$  are the two images to be compared.  $p(x)$  and  $p(y)$  are the marginal probability distribution functions of the gray values of  $X$  and  $Y$ .

They are defined as the normalized histograms for each of the two images.  $p(x,y)$  is the joint probability distribution function for the gray values of both images and is defined as the normalized two dimensional joint histogram of the images.

The higher the mutual information, the higher the probability that the two compared images are well aligned. To minimize the computational costs and get better results the mutual information is not calculated for the whole images but only at a discoidal region covering the whole candidate identified in the previous step (section 2). A reference image is chosen to which all other images are registered. This reference image is defined as the image at the time step where the heart was detected.

All other images, the so-called moving images, are placed on the reference image and shifted in both directions. The mutual information is calculated for every displacement. The shift that leads to the maximum mutual information is considered the optimal registration. The shift of the moving images is restricted by  $\pm 2r$  where  $r$  is the radius of the candidate.

## 4 Segmentation

After registration the final segmentation is performed: the goal is to detect the inner and outer boundaries of the myocardium in each time step. To separate myocardium from other tissues we exploit the fact that the contrast agent arrives at different times at different anatomical regions. In the first step characteristic intensity-time curves for four different regions (left ventricle, myocardium, right ventricle, and background) are calculated (section 4.1). In the second step these curves are used to derive contours for the individual time steps (section 4.2).

### 4.1 Estimation of Intensity-time Curves

In perfusion images four regions can be identified by their characteristic intensity-time curves: left ventricle, right ventricle, myocardium, and background. Four steps are carried out to estimate these curves: Initial Estimation, Classification, Classification Refinement, Final Estimation.

#### Initial Estimation

Based on the model fitted to the data in the localization step an initial estimate for the characteristic intensity-time curves is made.

The outline of the initially detected circular candidate (section 2) identifies pixels of the myocardium. By observing the intensities of these pixels over time an initial approximation of the characteristic intensity-time curve of the myocardium is set up (figure 4 (a)).

The intensity-time curve of the left ventricle is considered next. Therefore the pixels inside the circle defining

the myocardium are observed. It is not guaranteed that the whole inner area of this circle corresponds to the left ventricle. For a more robust estimation of the curve only pixels lying within a disc of half the myocardium's radius are used. Within this region fewer misleading pixels (as caused by papillary muscles) disturb the result. This leads to an initial characteristic intensity-time curve of the left ventricle (figure 4 (b)).

To estimate the intensity-time curve for the right ventricle a representative region has to be identified. To roughly locate the right ventricle the fact is used that contrast agent first appears in the right ventricle and then in the left ventricle. The appearance of the contrast agent causes significant increase of the gray value. The greatest intensity increase in subsequent time steps indicates the moment of contrast agent arrival. To locate the right ventricle a circular area outside the myocardium is selected and divided into eight segments. For every segment the intensity-time curve is determined. The largest increase of intensity before the contrast agent arrival in the left ventricle is calculated. The segment for which this increase is largest is considered to overlap with the right ventricle. The intensity-time curve of this segment is the representative curve of the right ventricle (figure 4 (c)).

The intensities of the background are assumed to be nearly constant over time. Therefore the characteristic curve of the background is defined as curve with a constant value.

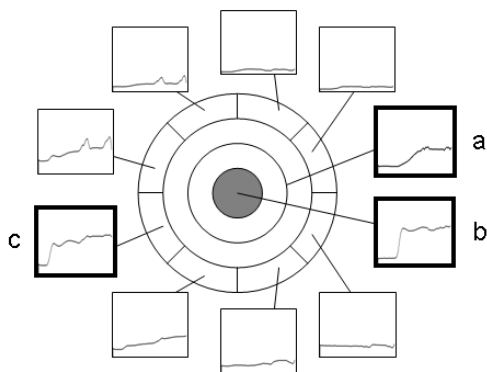


Figure 4: Example of segment curves. Pixels on the circle define the curve of the myocardium (a). Pixels inside the circle (gray area) define the curve of the left ventricle (b). Early contrast agent arrival reveals the segment representing the right ventricle (c).

### Classification

Pixels are classified as belonging either to the left ventricle, myocardium, right ventricle, or background. The intensity-time curves of individual pixels are examined therefore. The characteristic curve which is most similar defines the class of the pixel. Differences between curves are measured as the mean square error of the angles of the

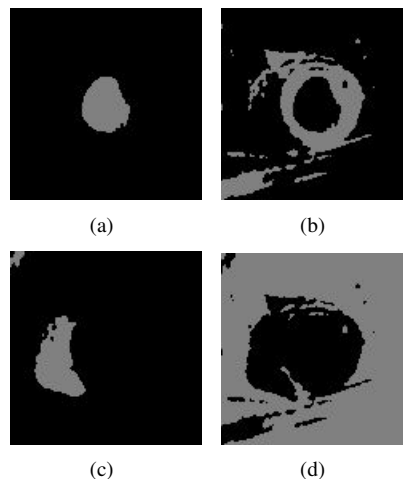


Figure 5: Initial classification. (a) Left Ventricle, (b) Myocardium, (c) Right Ventricle, (d) Background.

slopes. This measure is used to compensate for different intensity offsets. The pixel-wise classification results in four masks (figure 5).

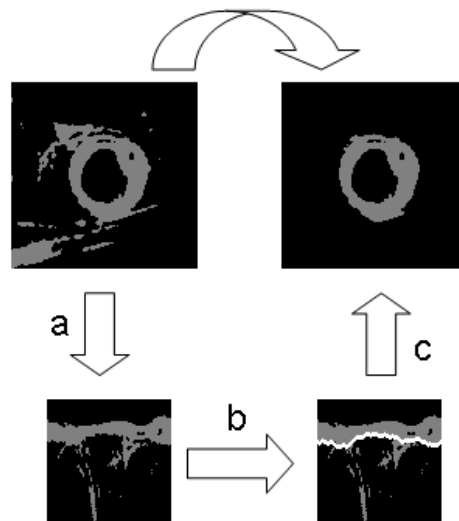


Figure 6: Optimization of the myocardial boundary. After transforming the mask into polar coordinates (a), the path with minimum costs (white curve) is determined (b) and then transformed back to the spatial domain (c).

### Classification Refinement

The masks from the previous step are refined.

The masks of left ventricle and right ventricle are refined by selecting their largest connected components.

The mask of the myocardium is refined as follows. The method for improving the contour is based on the branch-and-bound approach from Yeh et al. [21]. It is assumed that the outer contour of the myocardium has approxi-

mately a circular shape. The mask of the myocardium is transformed into polar coordinates (angle + radius)(figure 6 (a)). Every column identifies an angle and every row a radius. A perfectly circular boundary of the myocardium would appear as a straight horizontal line. To find an approximately circular curve a path going from left to right containing every column only once has to be found. To allow some shape variations the radius is allowed to change by one pixel between adjacent columns. To fulfill the constraint of a closed curve the first and last column are considered adjacent. To find the optimal curve weights are defined for every pixel. At a transition from the myocardium to a different type of tissue the weight is set to zero, from a different tissue to the myocardium to two and in all other cases to one. Then the path with minimum costs fulfilling the constraints is calculated (figure 6 (b)) and the optimized area is extracted (figure 6 (c)).

### Final Estimation

The characteristic intensity-time curves are re-estimated. This is done by observing pixels within the refined masks.

## 4.2 Boundary Extraction

After estimating the intensity-time curves the boundaries of the myocardium are calculated for each individual time step.

This is a challenge because depending on the progress of the contrast agent highly varying contrast is observed in different regions.

For the inner boundary of the myocardium there is low contrast between myocardium and left ventricle when the contrast agent has not yet reached the left ventricle (figure 1(a)) or when it appears in both areas (figure 1(d)). The contrast between myocardium and lung is very low before the contrast agent appears in the myocardium (figure 1 (a-c)). Additional, the contrast between the right ventricle and the myocardium is also very low at the first time steps (figure 1(a)).

Therefore the inner boundary is only clearly determined in time steps where the difference of the characteristic curves of left ventricle and myocardium is greater than a given threshold (10% of gray value range). At all other time steps a default boundary is assigned. The default boundary is determined at the time step with highest contrast between left ventricle and myocardium. This time step is derived from the characteristic curves of these regions. The outer boundary is determined for all time steps and further refined to deal with poor contrast.

To determine the boundaries the same algorithm as in the previous section (4.1) - finding a path with minimal costs - is used. However, the assignment of weights has to be done differently since individual time steps are considered now.

### Weights Definition

For each time step  $t$  the mean gray values  $\mu_{myo}(t)$  and  $\mu_{LV}(t)$  and standard deviations  $\sigma_{myo}(t)$  and  $\sigma_{LV}(t)$  for the regions of left ventricle and myocardium are calculated. This is done based on the optimized masks as determined in section 4.1. It is assumed that the distribution of gray values for myocardium and left ventricle follow a normal distribution. The intersection point  $intersection(t)$  of the curves representing those normal distributions is determined. Each image is thresholded keeping pixels within a specific gray value interval. The interval for thresholding is determined as:

$$interval(t) = \begin{cases} [\mu_{myo}(t) - \sigma_{myo}(t), intersection(t)], & \text{if } \mu_{myo}(t) \leq \mu_{LV}(t) \\ [intersection(t), \mu_{myo}(t) + \sigma_{myo}(t)], & \text{if } \mu_{myo}(t) > \mu_{LV}(t) \end{cases}$$

After thresholding each pixel of the image is assigned either myocardium (M) or other tissue (O). The thresholded image is transformed into polar coordinates. For detecting the boundary as shortest path weights are assigned to pixels. For the inner boundary the weights are defined as follows: M-M: 20, O-M: 5(n-1), M-O: 20, O-O: 10. Whereby n indicates the n-th transition from O to M in one column starting from the center of the left ventricle. This is used to penalize transitions which are further away from the center and therefore more unlikely correct transitions. For the outer boundary a transition of M to O a weight of zero and for all others a weight of 10 is assigned. To avoid intersections between the inner and outer boundary all pixels inside the inner boundary are assigned infinity.

### Outer Boundary Refinement

In a final step the outer boundaries are further refined. At equidistant angles the thickness of the myocardium is calculated. For every angle a mean thickness is calculated over time. The final outer boundary is then calculated by adding this mean thickness to the inner boundary. This proceeding is justified by the assumption that no contraction of the myocardium in the perfusion images is observed because the images are ECG-triggered.

## 5 Results

The presented method was tested on eleven cardiac perfusion MRI datasets from nine different patients and three different scanners. Five patients were imaged with a Philips Gyroscan 1.5T NT Intera with a resolution of  $128 \times 128$  voxels, three to five slices and 17 to 43 time steps. Two patients were imaged with a Siemens Symphony 1.5T with a resolution of  $208 \times 256$  voxels, only one slice and 60 time steps. Two patients were imaged under rest and stress conditions with a Philips 1.5T Intera with a resolution of  $256 \times 256$  voxels, three slices and 59 to 66 time steps.

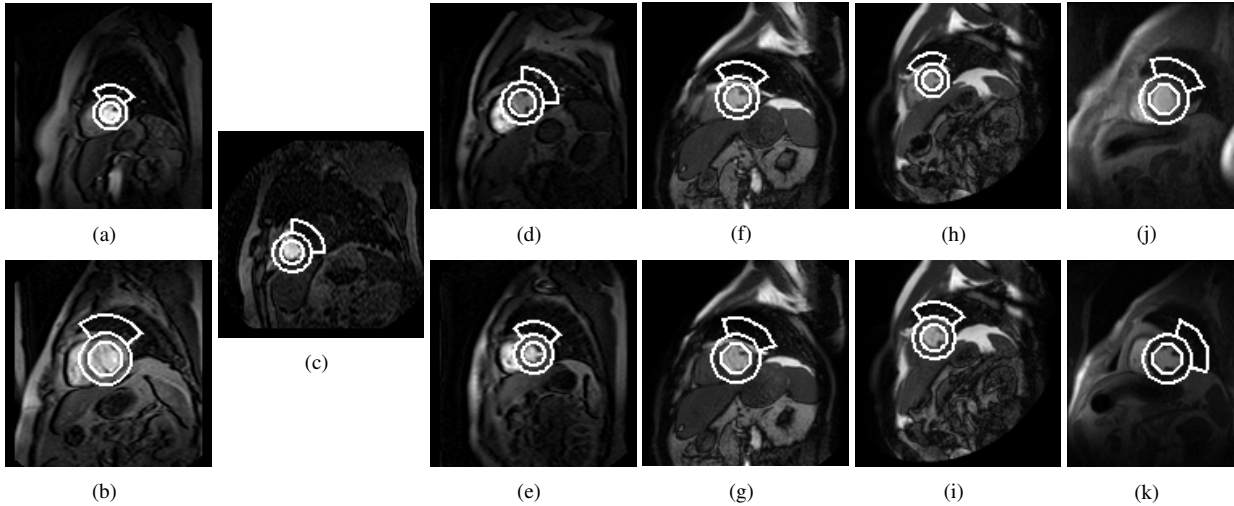


Figure 7: Model based ROI selection. Illustration of the best resulting candidates obtained by the automatic model based ROI selection applied to different datasets. Only (c) shows a wrong detection of the candidate: instead of the left ventricle the right ventricle was located. (a)-(e) Philips Gyroscan 1.5T NT Intera ( $128 \times 128$ ), (f)-(i) Philips 1.5T Intera ( $256 \times 256$ ) (acquired in rest (f), (h) and stress (g), (i) conditions), (j) and (k) Siemens Symphony 1.5T ( $208 \times 256$ ).

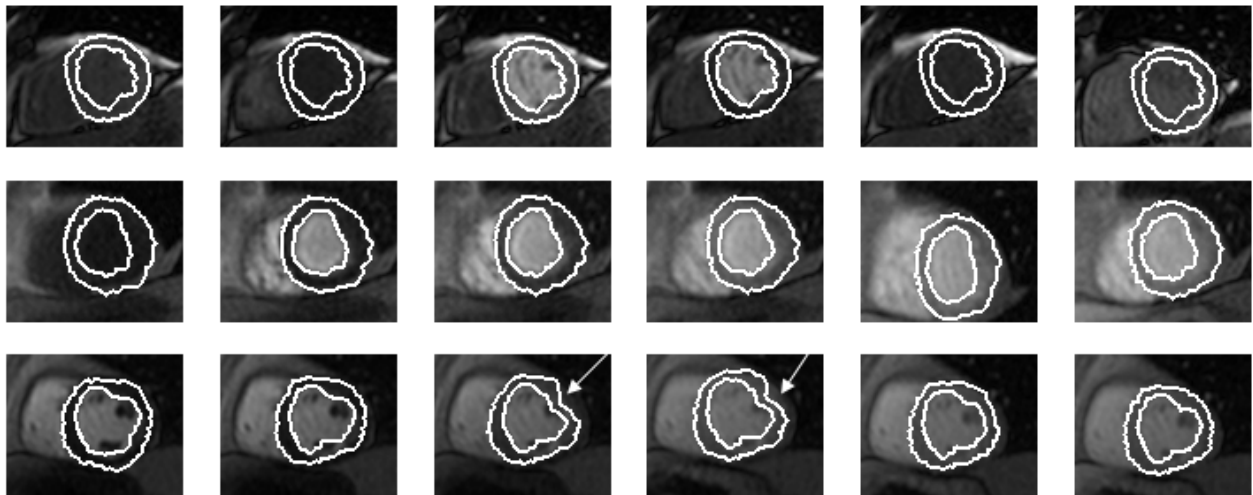


Figure 8: Segmentation. Some time steps of the segmentation of three different datasets. The lower row shows a dataset where the papillary muscles appear inside the myocardium (arrows).

The automatic ROI selection leads to quite stable results. In only one dataset a wrong candidate was detected (figure 7(c)) probably caused by irregular shape of the left ventricle and a poor resolution of  $128 \times 128$ .

The registration of the images works nearly perfect: The registration only failed at one single time step of a single patient study.

The segmentation leads to expected results (figure 8). The papillary muscles sometimes appear inside the myocardium and sometimes outside. In such cases the outer boundary of the myocardium may not reside - as expected - to the edges bordering the myocardium (lower row in figure 8).

## 6 Conclusions

A method was presented for fully automatic segmentation of cardiac perfusion MRIs. This method is designed to segment data from different scanners. This method includes selection of the region of interest, image registration, and segmentation of the myocardium. Experiments indicate that the method has a potential to become a solid basis for subsequent analysis. Currently no automatic perfusion analysis for the myocardium is supported by our system. This will be added in future work. We also plan to further improve the region of interest selection to obtain better segmentation results. Furthermore a refinement of the outer boundary extraction is planned.

## 7 Acknowledgment

This work has been carried out at the VRVis Research Center for Virtual Reality and Visualization in Vienna (<http://www.vrvis.at>) and is a part of my master thesis. The work was funded by AGFA Health Care. I want to thank Katja Bühler for the possibility to accomplish this master thesis. Special thanks goes to my advisors Jiří Hladůvka and Sebastian Zambal for their permanent encouragement helping with my work.

## References

- [1] G. Adluru, E. V. R. D. Bella, and R. T. Whitaker. Automatic segmentation of cardiac short axis slices in perfusion. In *ISBI*, pages 133–136, 2006.
- [2] N. Al-Saadi, E. Nagel, M. Gross, A. Bornstedt, B. Schnackenburg, and C. e. a. Klein. Noninvasive Detection of Myocardial Ischemia From Perfusion Reserve Based on Cardiovascular Magnetic Resonance. *Circulation*, 101:1379–1383, 2000.
- [3] J. Bogaert, S. Dymarkowski, and A. Taylor. *Clinical Cardiac MRI*. Springer, 2005.
- [4] D. T. Gering. Automatic Segmentation of Cardiac MRI. In *MICCAI (1)*, pages 524–532, 2003.
- [5] B. Kaiser, S. Globits, H. Mayr, M. Mittendorfer, and E. Salomonowitz. Myokardiale First-Pass-Perfusionsdiagnostik mittels Magnetresonanztomographie. *Journal für Kardiologie*, 10:26–31, 2003.
- [6] J. Milles, R. J. van der Geest, M. Jerosch-Herold, J. H. C. Reiber, and B. P. F. Lelieveldt. Fully Automated Registration of First-Pass Myocardial Perfusion MRI Using Independent Component Analysis. In *IPMI*, volume 4584, pages 544–555, 2007.
- [7] H. Ólafsdóttir. Registration and analysis of myocardial perfusion MRI. Master’s thesis, Informatics and Mathematical Modelling, Technical University of Denmark, DTU, 2004.
- [8] H. Ólafsdóttir. Nonrigid registration of myocardial perfusion MRI. In *Proc. Svenska Symposium i Bildanalys, SSBA 2005, Malmö, Sweden*, 2005.
- [9] C. Pluempitiwiriyaewej, J. M. F. Moura, Y.-J. L. Wu, and C. Ho. STACS: new active contour scheme for cardiac MR image segmentation. *IEEE Trans. Med. Imaging*, 24(5):593–603, 2005.
- [10] C. Pluempitiwiriyaewej and S. Sotthivirat. Active Contours With Automatic Initialization For Myocardial Perfusion Analysis. In *Engineering in Medicine and Biology Society*, pages 3332–3335, 2005.
- [11] W. Sörgel and V. Vaerman. Automatic heart localization from a 4D MRI dataset. In *SPIE Medical Imaging*, 1997.
- [12] L. Spreeuwiers, F. Wierda, and M. Breeuwer. Automatic correction of myocardial boundaries in MR cardio perfusion analysis. In *Computer Assisted Radiology and Surgery*, pages 902–907, 2002.
- [13] L. Spreeuwiers, F. Wierda, and M. Breeuwer. Optimal Myocardial Boundary Estimation for MR Cardio Perfusion Measurements Using Sensitivity Analysis. In *Computers in Cardiology*, pages 197–200, 2002.
- [14] M. Stegmann and H. Larsson. Motion-Compensation of Cardiac Perfusion MRI Using a Statistical Texture Ensemble. In *FIMH*, pages 151–161, 2003.
- [15] M. B. Stegmann, H. Ólafsdóttir, and H. B. W. Larsson. Unsupervised motion-compensation of multislice cardiac perfusion MRI. *Medical Image Analysis*, 9(4):394–410, 2005.
- [16] Y. Sun, M.-P. Jolly, and J. M. F. Moura. Contrast-Invariant Registration of Cardiac and Renal MR Perfusion Images. In *MICCAI (1)*, pages 903–910, 2004.
- [17] P. Viola and W. M. Wells. Alignment by maximization of mutual information. *International Journal of Computer Vision*, 24(2):137–154, 1997.
- [18] N. Wilke, M. Jerosch-Herold, Y. Wang, Y. Huang, B. Christensen, A. Stillman, K. Ugurbil, K. McDonald, and R. Wilson. Myocardial perfusion reserve: assessment with multisection, quantitative, first-pass MR imaging. *Radiology*, 204(2):373–84, 1997.
- [19] S. Wolff, J. Schwitter, R. Coulden, M. Friedrich, D. Bluemke, R. Biederman, E. Martin, A. Lansky, F. Kashanian, T. Foo, P. Licato, and C. Comeau. Myocardial First-Pass Perfusion Magnetic Resonance Imaging: A Multicenter Dose-Ranging Study. *Circulation*, 110:732–737, 2004.
- [20] K. Wong, E. Wu, M. Ng, Y. Wu, H. Tse, C. Lau, G. Lo, and E. Yang. Image Registration in Myocardial Perfusion MRI. *Engineering in Medicine and Biology Society, 2005. IEEE-EMBS 2005. 27th Annual International Conference of the*, 1:453–454, 2005.
- [21] J.-Y. Yeh, J. C. Fu, C. C. Wu, H. M. Lin, and J. W. Chai. Myocardial border detection by branch-and-bound dynamic programming in magnetic resonance images. *Computer Methods and Programs in Biomedicine*, 79(1):19–29, 2005.
- [22] S. Zambal, A. Schöllhuber, K. Bühler, and J. Hladůvka. Fast and Robust Localization of the Heart in Cardiac MRI Series. *VisApp*, 1:341–346, 2008.